Evaluation of hypericin-mediated photodynamic therapy in combination with angiogenesis inhibitor bevacizumab using *in vivo* fluorescence confocal endomicroscopy

Ramaswamy Bhuvaneswari*
Patricia S. P. Thong*
National Cancer Centre
Division of Medical Sciences
11 Hospital Drive
Singapore 169610 Singapore

Yik-Yuen Gan
Nanyang Technological University
National Institute of Education
Natural Sciences and Science Education
1 Nanyang Walk
Singapore 637616 Singapore

Khee-Chee Soo
National Cancer Centre
Division of Medical Sciences
11 Hospital Drive
Singapore 169610 Singapore

Malini Olivo
National Cancer Centre
Division of Medical Sciences
11 Hospital Drive
Singapore 169610 Singapore
    and
Biomedical Sciences Institutes
Singapore Bioimaging Consortium
11 Biopolis Way
#02–02 Helios, Singapore
    and
National University Ireland
School of Physics
University Road
Galway, Ireland

Abstract. Photodynamic therapy (PDT) is an alternative cancer treatment modality that offers localized treatment using a photosensitizer and light. However, tumor angiogenesis is a major concern following PDT-induced hypoxia as it promotes recurrence. Bevacizumab is a monoclonal antibody that targets vascular endothelial growth factor (VEGF), thus preventing angiogenesis. The combination of PDT with antiangiogenic agents such as bevacizumab has shown promise in preclinical studies. We use confocal endomicroscopy to study the antiangiogenic effects of PDT in combination with bevacizumab. This technique offers *in vivo* surface and subsurface fluorescence imaging of tissue. Mice bearing xenograft bladder carcinoma tumors were treated with PDT, bevacizumab, or PDT and bevacizumab combination therapy. In tumor regression experiments, combination therapy treated tumors show the most regression. Confocal fluorescence endomicroscopy enables visualization of tumor blood vessels following treatment. Combination therapy treated tumors show the most post-treatment damage with reduced cross-sectional area of vessels. Immunohistochemistry and immunofluorescence studies show that VEGF expression is significantly downregulated in the tumors treated by combination therapy. Overall, combining PDT and bevacizumab is a promising cancer treatment approach. We also demonstrate that confocal endomicroscopy is useful for visualization of vasculature and evaluation of angiogenic response following therapeutic intervention. © *2010 Society of Photo-Optical Instrumentation Engineers.* [DOI: 10.1117/1.3281671]

1 Introduction

Photodynamic therapy (PDT) is a cancer treatment modality that involves the retention of photosensitizers in neoplastic tissue and subsequent activation by light of appropriate wavelength, resulting in highly selective photodynamic destruction of tumor tissue. The evident advantages of PDT over chemotherapy and radiotherapy are its selective targeting, reduced toxicity that allows for repeated treatments,[1,2] and nonimmunosuppressive nature.[3] Though therapeutic responses are encouraging, nonhomogeneous light distribution during PDT, incomplete photosensitizer dosage, and tissue dynamics are some of the factors that affect[4] the efficacy of PDT. Therefore,

incomplete treatment causes oxidative stress, leading to hypoxia within the tumor tissue and triggers the release of angiogenic molecules, resulting in angiogenesis (Fig. 1). This is one of the causes of tumor recurrence that has sometimes been noticed following PDT.

Angiogenesis, the process whereby new capillaries are formed from existing vessels, is necessary for tumor growth, progression, and metastasis.[5] The process of tumor angiogenesis is mainly triggered by the release of proangiogenic factors such as VEGF that promote endothelial cell proliferation, migration, and tube formation.[6] Elevated levels of VEGF expression have been found in most human malignancies, including bladder carcinomas.[7,8] Studies have demonstrated that high expression of VEGF observed in solid tumors is correlated with poor clinical outcome.[9] Several groups including

---

*Authors contributed equally to this work.
Address all correspondence to: Malini Olivo, National Cancer Centre, Division of Medical Sciences, 11 Hospital Drive, Singapore 169610. Tel: 65-6436-8317; Fax: 65-63720161; E-mail: dmsmcd@nccs.com.sg
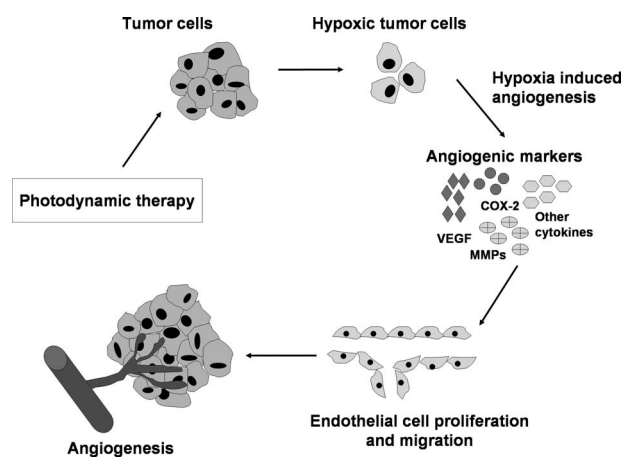
Fig. 1 Schematic diagram illustrating the events involved in PDT-activated angiogenesis. Treatment induced oxidative stress causes hypoxia within the tumor tissue, triggering the release of angiogenic growth factors that include vascular endothelial growth factor (VEGF), cyclooxygenase-2 (COX-2), matrix metalloproteinases (MMPs), and cytokines. These proangiogenic factors facilitate endothelial cell proliferation and migration, thus initiating angiogenesis and tumor growth.

ours[10–13] have reported the upregulation of VEGF following PDT. As VEGF and its receptors represent the central molecular targets for antiangiogenic intervention, this study proposes to test the efficacy of bevacizumab, an antiangiogenic agent, along with PDT. Bevacizumab is a recombinant, partially humanized, monoclonal antibody that binds to and inhibits the biologic activity of human VEGF, thus preventing interaction with its receptors. Bevacizumab when used along with conventional chemotherapy has shown antitumor activity in several cancer types with acceptable toxicity.[14,15] It has been approved for the treatment of colorectal cancer, non-small-cell lung cancer (NSCLC), breast cancer, prostate cancer, and renal cell carcinoma in many countries.[16] The relationship between PDT and angiogenesis was first established by Ferrario et al..[17] They demonstrated that the effectiveness of PDT treatment could be enhanced by combining it with angiogenic inhibitors. This study proposes to use bevacizumab along with PDT to improve the overall tumor responsiveness.

The evaluation of angiogenic responses in tumors to treatment regimes is highly important in the development of novel antiangiogenesis therapeutics. Structural and functional imaging of tumor vasculature has been studied using various imaging modalities including positron emission tomography (PET), magnetic resonance imaging (MRI), computed tomography (CT), ultrasound, and intravital microscopy.[18,19] In this study, we carried out *in vivo* fluorescence imaging of tumor blood vessels using laser confocal endomicroscopy to evaluate tumor vasculature status following treatment. Laser confocal endomicroscopy is an optical imaging technique that is capable of *in vivo* fluorescence imaging of surface and subsurface structures at the microscopic level.[20,21] Results were correlated to those from immunohistochemical (IHC) staining and immunofluorescence (IF) imaging for VEGF levels and overall tumor response from tumor regression study.

2 Materials and Methods

2.1 Cell Culture and Xenograft Tumor Model

Male Balb/c nude mice, 6 to 8 weeks of age, weighing an average of 24 to 25 g were obtained from the Animal Resource Centre (ARC), Western Australia. The epithelial human bladder carcinoma cell line (MGH-U1) was used to establish the xenograft model. The cells were cultured as a monolayer in RPMI-1640 medium supplemented with 10% fetal bovine serum (HyClone, Logan, Utah), 1% nonessential amino acids (Gibco, United States), 1% sodium pyruvate (Gibco, United States), and 100 units/ml penicillin/streptomycin (Gibco, United States) and incubated at 37 °C, 95% humidity, and 5% CO_2. Before inoculation, the cell layer was washed with phosphate-buffered saline (PBS), trypsinized, and counted using a hemocytometer. Approximately 3.0×10^6 MGH-U1 human bladder carcinoma cells suspended in 150 μl of Hanks' balanced salt solution (Gibco, United States) was injected subcutaneously into the lower flanks of the mice. The tumors were allowed to grow to sizes of 6 to 7 mm in diameter before PDT treatment was carried out, and the tumors were measured three times a week to assess tumor regression. Tumor volume was estimated by using the formula, volume $= (\pi/6 \times d1 \times d2 \times d3)$, where $d1$, $d2$, and $d3$ are tumor dimensions in three orthogonal directions. All procedures were approved by the Institutional Animal Care and Use Committee (IACUC), Singapore Health Services, Singapore, in accordance with international standards.

2.2 Photosensitizer

Hypericin was purchased from Molecular Probes, Oregon. A stock solution of 5 mg/ml hypericin was prepared by adding 200 μl of dimethyl sulfoxide (DMSO, Sigma Aldrich Inc, St Louis, Missouri) to 1 mg of hypericin. The stock solution was further diluted in DMSO and PBS (1:3 v/v) and injected intravenously into the tail vein based on the weight of the animal at a dosage of 5 mg/kg.

2.3 Treatment Protocol

Animals were randomly assigned to four different groups ($n = 10$) for treatment: (1) control (mice with untreated tumors), (2) PDT only, (3) bevacizumab only (without PDT), and (4) PDT in combination with bevacizumab. PDT involved the intravenous injection of hypericin, followed by illumination with a light source consisting of filtered halogen light (Zeiss KL1500) fitted with a customized 560 to 640-nm bandpass filter. Light irradiation was performed 6 h post hypericin administration. A light fluence of 120 J/cm² and irradiance rate of 100 mW/cm² was used to perform PDT. Bevacizumab was administered by multiple intraperitoneal injections (10 mg/kg) at time 0 (immediately after PDT), 24 h, 48 h, and then every other day up to 90 days post PDT (as previously described in Ferrario et al.[11]). Treated and control tumors were monitored three times per week to chart the growth rate.

2.4 Dosage of Bevacizumab (Avastin)

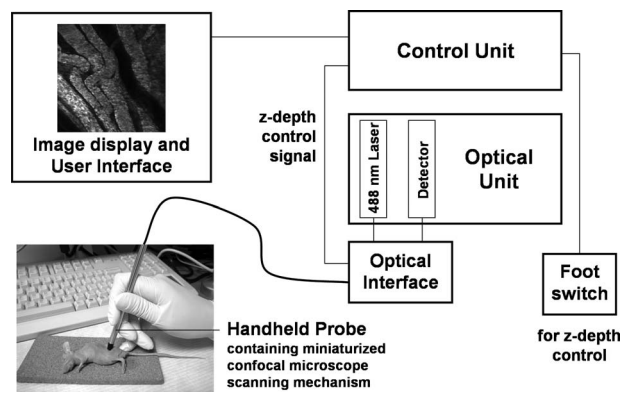A stock solution of concentration 25 mg/ml bevacizumab (Avastin™; Genentech, Inc., South San Francisco, California)

Fig. 2 Schematic diagram of the confocal endomicroscopy system with a handheld rigid probe used for *in vivo* fluorescence imaging of tumor vasculature in animal models.

was diluted with saline to prepare a working solution. It was administered intraperitonially at a dosage of 10 mg/kg.

2.5 Preparation of Mice for In Vivo Fluorescence Imaging

Fluorescein isothiocyanate (FITC)-labeled dextran [molecular weight (MW) 150 kDa, Sigma Aldrich, United States] solution was prepared at a concentration of 25 mg/ml. Then 10 μl FITC dextran per gram weight of the animal was injected intravenously. The nude mice were then anesthetized with a cocktail of Hypnorm (0.315 mg/ml fentanyl citrate and 10 mg/ml flanuisone, Janssen) and Dormicum (5 mg/ml midazolam HCl, David Bull Laboratories). The skin overlaying the tumor was carefully removed to expose the tumor.

2.6 Laser Confocal Endomicroscopy

In vivo fluorescence microscopic imaging of tumor blood vessels was carried out using a laser confocal endomicroscope approximately 30 min after intravenous administration of FITC dextran. Experiments were performed on the animals from day 25 to day 90, based on the maximum tumor volume limit or the completion of the treatment. We previously described the design of a prototype of the laser confocal endomicroscope in detail.[20] The new Optiscan FIVE 1 system (Optiscan Pty Ltd., Victoria, Australia) features the same basic design with improved specifications. A schematic diagram of the system is shown in Fig. 2. A 488-nm laser provides excitation for *in vivo* fluorescence microscopy of tissue with a lateral resolution of 0.7 μm and an axial resolution of 7 μm within a field of view of 475×475 μm. The excitation light is coupled into a single optical fiber that acts as both a point source and a point detection pinhole for confocal imaging. A handheld rigid probe (model RBK6315A) with a probe shaft of length 150 mm and diameter 6.3 mm houses the miniaturized components of the *x*-*y* scanning and *z* axis actuator. A footswitch enables the imaging depth to be controlled along the *z* axis range from the surface to 250 μm subsurface in 4-μm steps, as well as to facilitate image capture. Serial 1024×1024-pixels images can be acquired at a frame rate of 0.7 frames/s. For optimum image contrast, the laser power can be adjusted between 0 to 1000 μW at the 5.0-mm-diameter distal tip of the probe in contact with the

tissue. Fluorescence signals are collected via a 505 to 750-nm emission filter.

2.7 Endomicroscope Image Processing and Analysis

Blood vessel analysis was carried out using the Cell D imaging software (Olympus, Soft Imaging Solutions GmbH, Germany). The measurement function was used to measure the cross-sectional areas of the blood vessels visible within the field of view of the endomicroscope images by drawing user-defined regions of interest along the vessels. The mean vessel area for each animal group was calculated from images captured from three locations with high vessel density and that are between 20 and 40 μm below the surface of the tumor.

2.8 Immunohistochemistry

Processing of the samples was done using a tissue processor (Leica TP 1020, Germany). Briefly the tissue samples were fixed in 10% formalin for 24 h, and then processed in an ascending series of ethanol and subsequently cleared with xylene and embedded in paraffin. The paraffin-embedded samples of bladder tumors were cut at a thickness of 4 μm using a microtome (Leica RM 2135, Germany). The sections were mounted on superfrost/plus slides (Fischer Scientific, United States) and air-dried. On the day of staining, the slides were placed in 60 °C oven for 1 h and immersed in zylene for 10 min before rehydration in ethanol series. Sections were incubated in hydrogen peroxide for 10 min to block endogenous peroxidase activity. After which, the sections were incubated with VEGF (BD Biosciences Pharmingen, United States) primary antibody (1:100) for 1 h. To confirm the specificity of binding, normal mouse serum immunoglobulin G (IgG$_1$) (1:500) was used instead of primary antibody to serve as the negative control. Following extensive washing, sections were incubated for 30 min in the secondary biotinylated antibody followed by DAB Chromogen (Dako REAL EnVision Detection System, United States) for 10 min. Sections were then counterstained with Harris's hematoxylin and dehydrated in ascending grades of ethanol before being cleared in xylene and mounted under a cover slip. Images from the slides were captured using an image processing software (AxioVision v.4.6.3.0, Carl Zeiss Imaging Solutions, GmbH). The National Institutes of Health (NIH) Image J v1.62 software was used to analyze the images and quantify the expression of VEGF. Briefly, the percentage of positively stained cells was calculated by obtaining the area of the immunostained regions divided by the total area of the image. IHC scoring was performed based on the prevalence of CD31 staining within the tumor (no staining=0, <10% staining =1, 10 to 25%=2, 26 to 50%=3, 51 to 75%=4, and 76 to 100%=5).

2.9 Immunofluorescence

Fresh frozen tissue sections were fixed in 2% paraformaldehyde for 2 min. The specimens were blocked for 1 h with normal goat serum in Triton X-100 (BDH, United Kingdom). After blocking, sections were incubated overnight with VEGF mouse monoclonal antibody (Abcam, United Kingdom) at 4 °C. Nonimmune IgG was used as a control. After rinsing in PBS, the specimens were stained with FITC-conjugated sec-
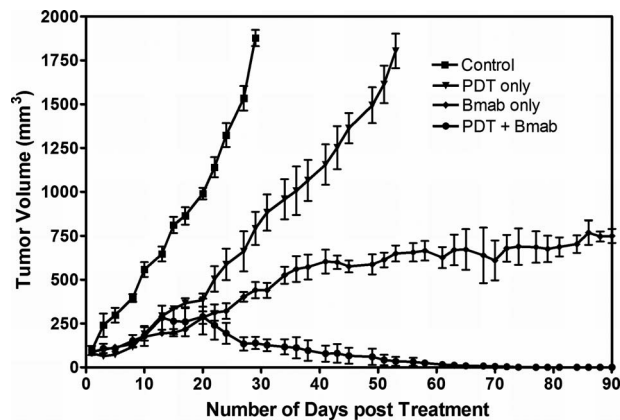
Fig. 3 Tumor volume charted against number of days posttreatment, to assess the tumor response in various treatment groups. The combination therapy group of PDT and bevacizumab (Bmab) exhibited the greatest tumor response in comparison with all other groups. Each group represents the mean response [bars, standard error (SE)] of 10 animals.

Fig. 4 Tumor blood vessels visualized approximately 30 min after intravenous administration of FITC-dextran in (a) control, (b) PDT only, (c) bevacizumab only, and (d) PDT and bevacizumab treated groups. Imaging was performed on the animals from day 25 to day 90, based on the maximum tumor volume limit or the completion of the antiangiogenesis treatment. Control blood vessels were well developed, dense, and intact while those in treated groups showed varying degrees of vessel damage following treatment. The PDT and bevacizumab combination treatment group showed the most posttreatment damage, with shrunken vessels and leaky vessel walls resulting in a diffuse fluorescence background.

ondary antibody for 2 h at room temperature in the dark. The slides were then rinsed with PBS and stained with DAPI for 30 min. Finally, the slides were rinsed and mounted with Vectashield® Mounting Medium (Vector Laboratories Inc., United States). IF images were captured using a laser confocal fluorescence microscope (Meta LSM 510, Carl Zeiss, Germany) and image analysis was performed using the ImageJ software (1.41o, W. Rasband, NIH, United States).

2.10 Statistical Analyses

Statistical analysis was performed using GraphPad Prism, version 4.0 (GraphPad Software, Inc., San Diego, California). A one-way analysis of variance (ANOVA) was used to analyze the variance. Dunnett's multiple comparison test was used to analyze the difference in mean vessel area between control and the other groups. Bonferroni's multiple comparison test was used to compare the significance between all the groups for tumor regression experiments. A p value of < 0.05 was considered to be significant.

3 Results

3.1 Tumor Regression

To investigate the long-term effectiveness of PDT in combination with bevacizumab, we induced MGH-U1 xenograft tumors in athymic nude mice models. Tumors were allowed to grow to sizes of 6 to 7 mm in diameter before PDT treatment was carried out and were measured three times a week and charted for 90 days (Fig. 3). A control IgG group was also evaluated. However, since the results were similar to the control tumors, they are not described in this paper. The mean tumor volume for each group of 8 to 10 animals is shown against the number of days post PDT. Tumor inhibition was calculated on day 29, when the control tumors reached a maximum volume of 2 cm³. Tumor inhibition of $85.8 \pm 1.5\%$ ($p < 0.001$) was observed in tumors treated with the combination therapy of PDT and bevacizumab in comparison to control tumors. A week after treatment, accelerated tumor growth was noticed in the combination therapy group, but
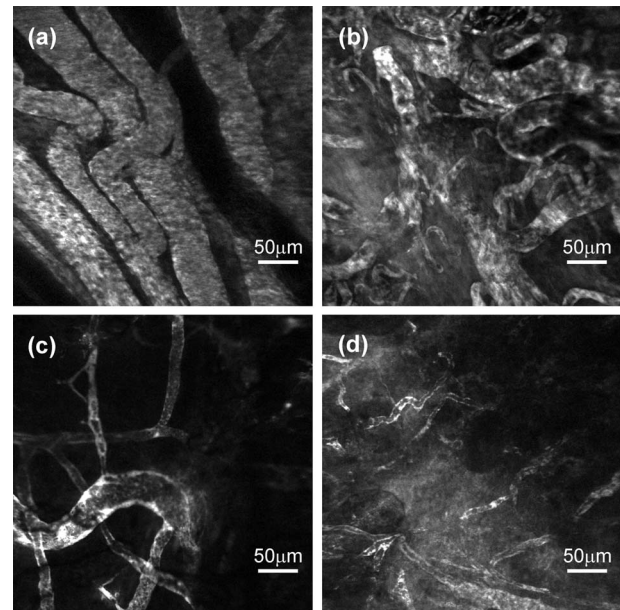
there was a decrease thereafter in tumor size, resulting in a permanent and complete tumor regression. The tumors treated with PDT only and bevacizumab only, exhibited $57.8 \pm 1.2\%$ ($p < 0.001$) and $76.5 \pm 1.8\%$ ($p < 0.001$) inhibition, respectively, compared to the control group. Compared to the control, the overall tumor response was greater in the monotherapy groups of PDT only and bevacizumab only. The treatment modalities in our study did not induce any signs of toxicity such as excessive weight loss, diarrhea, or vomiting in the animals. No treatment-related death occurred.

To further confirm the results from the tumor regression experiments, investigations were conducted at the vascular and molecular levels to determine the mechanism of the angiogenesis process following treatment.

3.2 Visualization of Tumor Vessel Using Laser Confocal Endomicroscopy

Tumor blood vessels were visualized using confocal endomicroscopy approximately 30 min after intravenous administration of FITC-dextran. Control [Fig. 4(a)] blood vessels were well developed, dense, and intact while those in treated groups [Figs. 4(b)–4(d)] showed varying degrees of vessel damage following treatment. Tumors treated with bevacizumab only exhibited lower vessel density; however, normalized morphology was noticed in the remaining blood vessels that could possibly allow blood flow to tumors. The PDT and bevacizumab combination treatment group showed the most
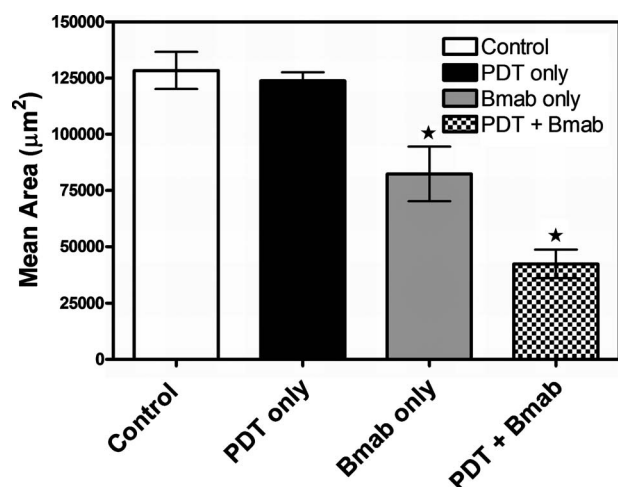
Fig. 5 Graph depicting the mean vessel area in the different treatment groups. A 1.3-fold decrease of vessel area was observed in bevacizumab only group, while the PDT and bevacizumab (Bmab) combination therapy group exhibited threefold reduction in mean vessel area compared to the control group.

Fig. 6 VEGF expression assessed in tumor sections using immunohistochemistry. The brown-colored regions in the images indicate VEGF staining in (a) control, (b) PDT only, (c) bevacizumab only, and (d) PDT and bevacizumab treated tumors. Maximum VEGF staining of 28 to 30% (IHC score 3) was noticed in the cytoplasm of PDT and control tumors. Around 16% (IHC score 2) concentrated staining was observed in the bevacizumab only group, and light staining of 6% (IHC score 1) was found in the combination therapy group.

posttreatment damage, with shrunken vessels and leaky vessel walls resulting in a diffuse fluorescence background.

3.3 Analysis of Mean Vessel Area

Mean vessel areas were calculated from the endomicroscope images of the tumors. Compared to the control group, a 1.3-fold decrease in mean vessel area ($p < 0.05$) was observed in the bevacizumab-only group and a three-fold reduction of vessel area ($p < 0.01$) was noticed in the PDT and bevacizumab combination therapy group (Fig. 5).

3.4 Detection of VEGF in Tumor Tissue Using Immunohistochemistry and IF

VEGF expression was assessed in the xenograft bladder tumor model using immunohistochemistry and IF techniques. All of the tumors exhibited cytoplasmic staining for VEGF. Maximum VEGF staining of 27 to 31% (IHC score 3) was noticed in PDT only and control tumor tissue. Around 16 to 20% (IHC score 2) scattered staining in certain regions of the cytoplasm was observed in the bevacizumab-only treated group and light staining of 6 to 8% (IHC score 1) was found in the combination therapy group (Figs. 6 and 7).

4 Discussion

PDT is a promising alternative cancer treatment modality that has the advantage of being nonimmunosupressive, unlike other conventional therapies. However, one of its potential drawbacks is post-PDT angiogenesis. Angiogenesis, the formation of blood vessels, is a multistep process that is essential for tumor growth and progression. It is one of the known causes of tumor regrowth in PDT-treated tumors.[17,22]. Since, VEGF is one of the most important proangiogenic growth factors that plays a pivotal role in the regulation of angiogenesis post PDT,[23] targeting tumor blood vessels in combination with PDT is a promising approach for cancer treatment. We demonstrated the use of angiogenesis inhibitor bevacizumab in combination with PDT to block the VEGF signaling path-
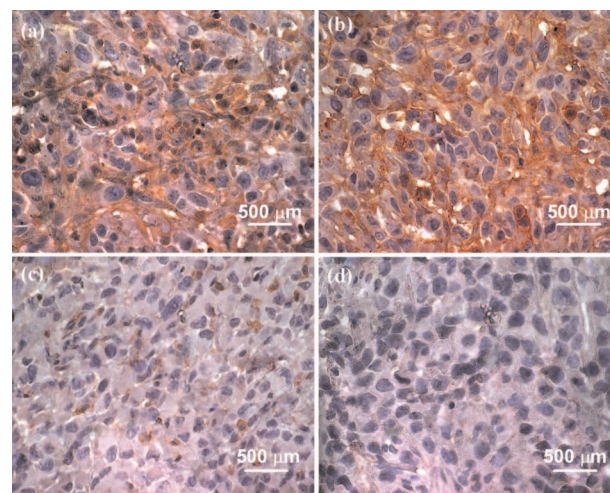
way and to eventually achieve long-term tumor control. We previously compared high- and low-dose PDT in combination with bevacizumab.[22] In this experiment, an acute PDT regime with a light dose of 120 J/cm^2 and a fluence rate of 100 mW/cm^2 was administered. A high fluence rate depletes tumor oxygen to a great extent during treatment, thereby reducing the primary cytotoxic processes of PDT and affecting tumor control.[24,25] High-fluence-rate PDT was used in this
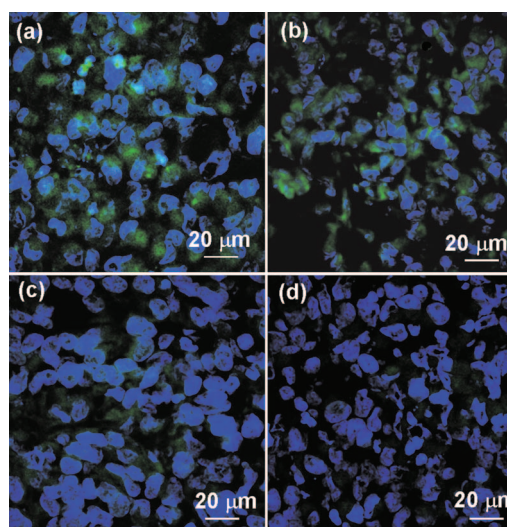

Fig. 7 IF was performed to confirm the immunohistochemistry results. In the confocal images, the green FITC fluorescence staining indicates the expression of VEGF. Intense staining of 27 to 31% was observed in (a) control and (b) PDT only groups; and 8% staining were recorded in the (c) bevacizumab only and (d) PDT and bevacizumab groups, respectively. The results obtained from IHC and IF staining techniques were comparable for all the groups.

study to test our hypothesis that combining PDT and bevacizumab can improve tumor control and also to evaluate the effectiveness of bevacizumab to inhibit VEGF. However, note that variations in PDT protocol such as low-dose PDT, fractionated PDT, vascular-mediated PDT, and PDT using long drug-light intervals have shown to be effective in controlling tumor recurrence.[22,26–28] We also utilized laser confocal endomicroscopy to visualize blood vessels and evaluate tumor response.

Our tumor regression data demonstrated that combining PDT and bevacizumab can impede the angiogenic process and improve the response of treated tumors. The tumor volume of the PDT-treated group was significantly greater than the bevacizumab-treated and combination-therapy-treated groups as the high fluence rate used during treatment can deplete tumor oxygen to a large extent, releasing stress-induced survival molecules that reduce the effectiveness of PDT and affect tumor control.[29] Although tumor regression was also observed in bevacizumab-only treated groups, complete cure was not observed. Thus, targeting VEGF alone might not be sufficient to cause regression of most bulky tumors. One of the possible explanations for this observation may be related to pericytes that respond to angiogenic stimuli, promote endothelial stability through matrix deposition, and have macrophage-like function.[30] Complete cure was observed in tumors treated with PDT and continued bevacizumab therapy. Thus, our data supports the hypothesis that bevacizumab is capable of binding and neutralizing secreted VEGF, causing regression of tumor vessels, normalizing surviving mature vasculature, and preventing tumor recurrence.[15]

Further investigations at the vascular and molecular levels provided insight on the status of vasculature and VEGF in treated tumors. Laser confocal endomicroscopy offers *in vivo* surface and subsurface fluorescence imaging of tissue.[31] This technique has been used to examine different types of tissue and diseases, facilitating early diagnosis.[20,32,33] It has also been successfully used for *in vivo* visualization of blood vessels and blood flow.[34] The goal of this study was to visualize changes in the morphology and functionality of tumor vasculature to evaluate the efficacy of the antiangiogenic therapy. Blood vessels in control tumors were observed to be intact and dense, and the supply of nutrients delivered by such effective networks of blood vessels could have enhanced the proliferation of control tumors. Angiogenesis was noticed in the PDT-only treated group. This could be due to the release of proangiogenic factors by hypoxic tumor cells in response to PDT-induced stress. The results from this experiment revealed that the fluence rate of $100~\text{mW}/\text{cm}^2$ was high enough to induce oxidative stress, leading to hypoxia, thus promoting angiogenesis.

Decreased tumor vessel area and intact vasculature were observed in tumors treated with bevacizumab only. This observation may be similar to the "normalization" of vessels reported by Fukumura and Jain in preclinical and clinical models.[35] Numerous studies by this group[36–38] reported that administration of angiogenic inhibitors regulates the proangiogenic and antiangiogenic balance and restores the function and structure of the remaining vessels, thus allowing blood flow to the tumor. Therefore, when angiogenic inhibitors are combined with chemotherapy, improved blood flow would facilitate enhanced delivery of chemotherapy drugs. Optimal

results were obtained in the combination therapy group of PDT and bevacizumab, in which the vessels were leaky and functional alterations were also observed. Moreover, the mean vessel area was the lowest compared to the other groups. Therefore, we hypothesize that PDT-induced tumor damage was sustained by the regular administration of bevacizumab and by inhibiting the production of angiogenic growth factors, most importantly VEGF. This is in agreement with our earlier study, in which we reported that bevacizumab not only downregulated VEGF but also suppressed other growth factors such as angiogenin, basic fibroblast growth factor (bFGF), epidermal growth factor (EGF), and interleukins (IL-6 and IL-8) (Ref. 22).

Immunohistochemistry was performed to detect VEGF and IF was carried out to confirm the results. These are reliable methods that have been employed to validate VEGF expression.[39,40] As VEGF is a secreted protein, it was observed mainly in the cytoplasm and the extracellular matrix. As a response to increased hypoxia, greater amount of VEGF expression could have been observed in control and PDT-only-treated tumors.[17] Our data also suggests a reduction in VEGF concentrations in the combination therapy group, and this result is consistent with a study reported by Gomer et al. that demonstrated downregulation of VEGF in Kaposi's sarcoma by combining PDT and bevacizumab.[29]

5 Conclusion

In summary, our results show that combining PDT and bevacizumab is a promising approach for cancer therapy, in agreement with previous preclinical studies involving angiogenesis inhibitor combination therapies. When researching tumor angiogenesis, a crucial role is played by the use of imaging tools and the use of laboratory animals to simulate tumor growth and metastasis, both of which facilitate the evaluation of therapeutic targets. We demonstrated that by using laser confocal endomicroscopy, responses to antiangiogenic therapies can be evaluated successfully by *in vivo* imaging of tumor vasculature. Our preclinical results can pave the way to a successful translation to future clinical application of PDT and antiangiogenesis combination therapy.

References

1. D. E. Dolmans, D. Fukumura, and R. K. Jain, "Photodynamic therapy for cancer," *Nat. Rev. Cancer* **3**(5), 380–387 (2003).
2. I. J. Macdonald and T. J. Dougherty, "Basic principles of photodynamic therapy," *J. Porphyr. Phthalocyanines* **5**, 105–129 (2001).
3. A. P. Castano, P. Mroz, and M. R. Hamblin, "Photodynamic therapy and anti-tumour immunity," *Nat. Rev. Cancer* **6**(7), 535–545 (2006).
4. B. W. Henderson and V. H. Fingar, "Relationship of tumor hypoxia and response to photodynamic treatment in an experimental mouse tumor," *Cancer Res.* **47**(12), 3110–3114 (1987).
5. J. Folkman, "Role of angiogenesis in tumor growth and metastasis," *Semin. Oncol.* **29**(6, Suppl. 16), 15–18 (2002).
6. N. Ferrara, "Role of vascular endothelial growth factor in the regu-

lation of angiogenesis," *Kidney Int.* **56**(3), 794–814 (1999).

7. Z. M. Shao and M. Nguyen, "Angiogenic factors and bladder cancer," *Front. Biosci.* **7**, e33–35 (2002).

8. C. C. Yang, K. C. Chu, and W. M. Yeh, "The expression of vascular endothelial growth factor in transitional cell carcinoma of urinary bladder is correlated with cancer progression," *Semin Urol. Oncol.* **22**(1), 1–6 (2004).

9. H. Sasano and T. Suzuki, "Pathological evaluation of angiogenesis in human tumor," *Biomed. Pharmacother* **59**(Suppl. 2), S334–336 (2005).

10. R. Bhuvaneswari, Y. Y. Gan, K. K. Yee, K. C. Soo, and M. Olivo, "Effect of hypericin-mediated photodynamic therapy on the expression of vascular endothelial growth factor in human nasopharyngeal carcinoma," *Int. J. Mol. Med.* **20**(4), 421–428 (2007).

11. A. Ferrario and C. J. Gomer, "Avastin enhances photodynamic therapy treatment of Kaposi's sarcoma in a mouse tumor model," *J. Environ. Pathol. Toxicol. Oncol.* **25**(1–2), 251–259 (2006).

12. M. Uehara, T. Inokuchi, K. Sano, and W. ZuoLin, "Expression of vascular endothelial growth factor in mouse tumours subjected to photodynamic therapy," *Eur. J. Cancer* **37**(16), 2111–2115 (2001).

13. K. K. Yee, K. C. Soo, and M. Olivo, "Anti-angiogenic effects of hypericin-photodynamic therapy in combination with Celebrex in the treatment of human nasopharyngeal carcinoma," *Int. J. Mol. Med.* **16**(6), 993–1002 (2005).

14. J. M. Davies and R. M. Goldberg, "First-line therapeutic strategies in metastatic colorectal cancer," *Oncology* **22**(13), 1470–1479 (2008).

15. Y. Fujita, R. Abe, and H. Shimizu, "Clinical approaches toward tumor angiogenesis: past, present and future," *Curr. Pharm. Des.* **14**(36), 3820–3834 (2008).

16. T. Shih and C. Lindley, "Bevacizumab: an angiogenesis inhibitor for the treatment of solid malignancies," *Clin. Ther.* **28**(11), 1779–1802 (2006).

17. A. Ferrario, K. F. von Tiehl, N. Rucker, M. A. Schwarz, P. S. Gill, and C. J. Gomer, "Antiangiogenic treatment enhances photodynamic therapy responsiveness in a mouse mammary carcinoma," *Cancer Res.* **60**(15), 4066–4069 (2000).

18. N. Charnley, S. Donaldson, and P. Price, "Imaging angiogenesis," *Methods Mol. Biol.* **467**, 25–51 (2009).

19. D. Fukumura and R. K. Jain, "Imaging angiogenesis and the microenvironment," *APMIS* **116**(7–8), 695–715 (2008).

20. P. S. Thong, M. Olivo, K. W. Kho, W. Zheng, K. Mancer, M. Harris, and K. C. Soo, "Laser confocal endomicroscopy as a novel technique for fluorescence diagnostic imaging of the oral cavity," *J. Biomed. Opt.* **12**(1), 014007 (2007).

21. H. Liu, Y. Q. Li, T. Yu, Y. A. Zhao, J. P. Zhang, J. N. Zhang, Y. T. Guo, X. J. Xie, T. G. Zhang, and P. V. Desmond, "Confocal endomicroscopy for *in vivo* detection of microvascular architecture in normal and malignant lesions of upper gastrointestinal tract," *J. Gastroenterol. Hepatol* **23**(1), 56–61 (2008).

22. R. Bhuvaneswari, G. Y. Yuen, S. K. Chee, and M. Olivo, "Hypericin-mediated photodynamic therapy in combination with Avastin (bevacizumab) improves tumor response by downregulating angiogenic proteins," *Photochem. Photobiol. Sci.* **6**(12), 1275–1283 (2007).

23. R. Bhuvaneswari, Y. Y. Gan, K. C. Soo, and M. Olivo, "The effect of photodynamic therapy on angiogenesis," *Cell. Mol. Life Sci.* **66**(14), 2275–2283 (2009).

24. B. W. Henderson, S. O. Gollnick, J. W. Snyder, T. M. Busch, P. C. Kousis, R. T. Cheney, and J. Morgan, "Choice of oxygen-conserving treatment regimen determines the inflammatory response and outcome of photodynamic therapy of tumors," *Cancer Res.* **64**(6), 2120–2126 (2004).

25. H. W. Wang, M. E. Putt, M. J. Emanuele, D. B. Shin, E. Glatstein, A. G. Yodh, and T. M. Busch, "Treatment-induced changes in tumor oxygenation predict photodynamic therapy outcome," *Cancer Res.* **64**(20), 7553–7561 (2004).

26. E. R. de Haas, B. Kruijt, H. J. Sterenborg, H. A. Martino Neumann, and D. J. Robinson, "Fractionated illumination significantly improves the response of superficial basal cell carcinoma to aminolevulinic acid photodynamic therapy," *J. Invest. Dermatol.* **126**(12), 2679–2686 (2006).

27. R. Bhuvaneswari, Y. Y. Gan, S. S. Lucky, W. W. Chin, S. M. Ali, K. C. Soo, and M. Olivo, "Molecular profiling of angiogenesis in hypericin mediated photodynamic therapy," *Mol. Cancer* **7**, 56 (2008).

28. P. S. Thong, F. Watt, M. Q. Ren, P. H. Tan, K. C. Soo, and M. Olivo, "Hypericin-photodynamic therapy (PDT) using an alternative treatment regime suitable for multi-fraction PDT," *Photochem. Photobiol. Sci.* **82**(1), 1–8 (2006).

29. C. J. Gomer, A. Ferrario, M. Luna, N. Rucker, and S. Wong, "Photodynamic therapy: combined modality approaches targeting the tumor microenvironment," *Lasers Surg. Med.* **38**(5), 516–521 (2006).

30. C. Lu, A. A. Kamat, Y. G. Lin, W. M. Merritt, C. N. Landen, T. J. Kim, W. Spannuth, T. Arumugam, L. Y. Han, N. B. Jennings, C. Logsdon, R. B. Jaffe, R. L. Coleman, and A. K. Sood, "Dual targeting of endothelial cells and pericytes in antivascular therapy for ovarian carcinoma," *Clin. Cancer Res.* **13**(14), 4209–4217 (2007).

31. A. Hoffman, M. Goetz, M. Vieth, P. R. Galle, M. F. Neurath, and R. Kiesslich, "Confocal laser endomicroscopy: technical status and current indications," *Endoscopy* **38**(12), 1275–1283 (2006).

32. H. Liu, Y. Q. Li, T. Yu, Y. A. Zhao, J. P. Zhang, X. L. Zuo, C. Q. Li, J. N. Zhang, Y. T. Guo, and T. G. Zhang, "Confocal laser endomicroscopy for superficial esophageal squamous cell carcinoma," *Endoscopy* **41**(2), 99–106 (2009).

33. R. W. Leong, N. Q. Nguyen, C. G. Meredith, S. Al-Sohaily, D. Kukic, P. M. Delaney, E. R. Murr, J. Yong, N. D. Merrett, and A. V. Biankin, "*In vivo* confocal endomicroscopy in the diagnosis and evaluation of celiac disease," *Gastroenterology* **135**(6), 1870–1876 (2008).

34. M. Goetz, S. Thomas, A. Heimann, P. Delaney, C. Schneider, M. Relle, A. Schwarting, P. R. Galle, O. Kempski, M. F. Neurath, and R. Kiesslich, "Dynamic imaging of microvasculature and perfusion by miniaturized confocal laser microscopy," *Eur. Surg. Res.* **41**(3), 290–297 (2008).

35. D. Fukumura and R. K. Jain, "Tumor microvasculature and microenvironment: targets for anti-angiogenesis and normalization," *Microvasc. Res.* **74**(2–3), 72–84 (2007).

36. D. G. Duda, T. T. Batchelor, C. G. Willett, and R. K. Jain, "VEGF-targeted cancer therapy strategies: current progress, hurdles and future prospects," *Trends Mol. Med.* **13**(6), 223–230 (2007).

37. R. K. Jain, "Normalization of tumor vasculature: an emerging concept in antiangiogenic therapy," *Science* **307**(5706), 58–62 (2005).

38. R. K. Jain, R. T. Tong, and L. L. Munn, "Effect of vascular normalization by antiangiogenic therapy on interstitial hypertension, peritumor edema, and lymphatic metastasis: insights from a mathematical model," *Cancer Res.* **67**(6), 2729–2735 (2007).

39. H. Saito, S. Tsujitani, A. Kondo, M. Ikeguchi, M. Maeta, and N. Kaibara, "Expression of vascular endothelial growth factor correlates with hematogenous recurrence in gastric carcinoma," *Surgery (St. Louis)* **125**(2), 195–201 (1999).

40. M. Nakamura, H. Yamabe, H. Osawa, N. Nakamura, M. Shimada, R. Kumasaka, R. Murakami, T. Fujita, T. Osanai, and K. Okumura, "Hypoxic conditions stimulate the production of angiogenin and vascular endothelial growth factor by human renal proximal tubular epithelial cells in culture," *Nephrol. Dial Transplant* **21**(6), 1489–1495 (2006).